  Bull. Chem. Soc. Jpn., 61, 1323—1329 (1988)

Equilibrium and Kinetic Studies of the Interaction between Orange I and Bovine Serum Albumin

Kiyofumi MURAKAMI
Department of Chemistry, Faculty of Science, Yamaguchi University, Yoshida 1677-1, Yamaguchi 753
(Received July 20, 1987)

The interaction between Orange I (sodium 4-[(4-hydroxy-1-naphthalenyl)azo]benzenesulfonate) and bovine serum albumin (BSA) at pH=7.0 and 25 °C has been studied by equilibrium dialysis, spectrophotometry, and the temperature-jump method. Equilibrium dialysis has revealed the existence of sixteen equivalent binding sites with the binding constant of $K=9.7\times10^3$ M^{-1}. All of them were found to be equivalent also in the sense of spectrophotometry. That is, Orange I interacts with BSA in a typically nonspecific manner. Five relaxations were found by the temperature-jump measurements. These relaxation times, distributed over the time range from 10 μs to 0.1 s, were determined over a wide range of reactant concentrations. The fastest relaxation becomes slow, but the four slower ones become fast, with the increase in the concentration of the free ligand. The data were interpreted by means of a combination of the bimolecular binding processes and the four isomerization modes of BSA. The results were discussed in the light of the role of the configurational adaptability of albumin molecules in the ligand-binding mechanism.

A unique property of serum albumin is its capacity to bind reversibly a variety of ions and organic molecules, such as metal ions, fatty acids, bilirubin, hormones, amino acids, and drugs. This enables albumin molecules to play their inherent role as the carrier and the reservior of those ligands in blood. The physicochemical origin of this unique property has been thought attributable to (1) configurational adaptability:[1] binding sites on albumin molecule can assume a large number of configurations in equilibrium with each other and can, in the presence of a ligand, adopt the configuration which is most suitable for interaction or to (2) pronounced flexibility:[2] a ligand molecule, during the binding process, is able to modify the configuration of a binding region in such a way that a greater congruence between the ligand molecule and parts of the region is achieved.

In recent years, many kinetic studies of albumin-ligand binding have been performed in order to elucidate the binding mechanism.[3-8] The general conclusion of these studies is that the ligand binding occurs through several steps: the first step is probably the diffusion-controlled bimolecular binding reaction, while the subsequent ones are the stabilization processes of the complex. This conclusion seems to be in harmony with the concept of the pronounced flexibility of albumin molecules. However, the kinetic studies have been concerned only with specific ligands which have one or few strong primary sites and several weak secondary sites and with a concentration range where only primary bindings occur. If nonspecific ligands, which have only one kind of relatively weak binding site, are used, we may obtain different features of the ligand-binding mechanism of albumin molecules.

The present paper will describe the equilibrium and the kinetics of the interaction between Orange I and bovine serum albumin (BSA) and will suggest that the configurational adaptability is also operative for albumin-ligand binding.

Experimental

Materials. The albumin (fraction V from bovine serum) was purchased from Armour and was defatted by means of charcoal treatment in an acid solution,[9] lyophilized, and stored at 4 °C. The molar concentration of BSA was determined from the absorbance at 280 nm ($E^{1\%}_{1cm}=6.6$[10]), assuming the molecular weight of 67000. The Orange I (sodium 4-[(4-hydroxy-1-naphthalenyl)azo]benzenesulfonate) was purchased from Wako Pure Chemical Industries, purified by repeated recrystallization from sodium acetate and aqueous ethanol solutions, and dried at 110 °C in a vacuum for 20 hours. All the other chemicals used were reagent-grade. All the sample solutions were prepared in a 0.1 M† phosphate buffer at pH=7.00±0.02.

Methods. The extent of binding was determined by the use of the equilibrium dialysis technique. Visking dialysis tubing (24/32) cut to a length of 9 cm was treated with a 1% $NaHCO_3$ aqueous solution at 100 °C for 60 min, soaked in a 0.3% EDTA solution, and then exhaustively rinsed with distilled water. 5 ml of the BSA solution ([BSA]=5×10^{-5} M) placed inside the dialysis tubing was dialysed against 10 ml of the dye solution at 25 °C for 24 h. After equilibration, the concentration of the Orange I solution was determined spectrophotometrically using a molar-extinction coefficient, $\varepsilon_{475}=3.24\times10^4$ $M^{-1}cm^{-1}$.

The spectrophotometric measurements were carried out with Shimadzu UV-200S and UV-100 spectrophotometers.

The kinetic experiments were performed with a Unisoku TF-102 fluorescence temperature-jump spectrophotometer. The details of the apparatus have been reported elsewhere.[11] The data were obtained at the temperature-rise intervals of 5 °C. All the experiments were performed at 25±0.2 °C.

Results and Discussion

Binding Parameters. Figure 1 illustrates a Scatchard plot[12] of the interaction of Orange I with BSA at pH=7.0 and 25 °C. The well-defined linearity of the plot shows that the binding sites of Orange I on BSA can be regarded as identical and independent. The binding parameters for the interaction were determined using the Scatchard equation:

† 1 M=1 mol dm^{-3}.

$$\frac{\bar{\nu}}{L} = nK - \bar{\nu}K \quad (1)$$

where $\bar{\nu}$ is the number of moles of the ligand bound per molecule of the protein, L is the free ligand concentration, and n and K are the number of binding sites and the association constant respectively. n and K were determined from the slope and the intercept of the plot as n=15.6 and K=9.7×10^3 M^{-1}. That is, Orange I binds nonspecifically to sixteen sites on BSA.

Spectrophotometric Titration. Figure 2 shows the absorption spectra of Orange I in the presence of BSA at several concentrations. The absorbance around 475 nm is reduced with the increase in the concentration of BSA, showing approximate isosbestic points at 415 nm and 525 nm. The existence of the isosbestic points suggests the following equilibrium between free and bound forms of the ligand:

$$\mathbf{L} + \mathbf{S} \rightleftharpoons \mathbf{C} \quad (2)$$

where **L**, **S**, and **C** denote the free ligand, the free binding site, and the complex between them respectively. The apparent molar-extinction coefficient at a given wavelength can be expressed by:

$$\varepsilon = (\varepsilon_F - \varepsilon_B)\alpha + \varepsilon_B \quad (3)$$

where ε_F and ε_B are the molar-extinction coefficients of the free and bound ligands respectively and where α is the free fraction of the ligand. α can be estimated from n, K, and the initial concentrations of the ligand and the protein (L_0 and P_0) as:

$$\alpha = \frac{-\{K(nP_0 - L_0)\} + [\{K(nP_0 - L_0)\}^2 + 4KL_0]^{1/2}}{2KL_0} \quad (4)$$

If all the sixteen sites determined by the equilibrium dialysis contribute equally to the spectral change (Fig. 2), the ε vs. α plot (Eq. 3) must be a straight line, and the ε_B's, which can be determined independently from the slope and the intercept of the plot, must agree with each other. The plots shown in Fig. 3 for 460, 475, and 490 nm indicate a good linearity. Furthermore, the values of ε_B (ε_{460}=1.96×10^4 M^{-1}cm^{-1}, ε_{475}=2.15×10^4 M^{-1}cm^{-1}, and ε_{490}=2.08×10^4 M^{-1}cm^{-1}) determined from the slope agree well with those (ε_{460}=1.94×10^4 M^{-1}cm^{-1}, ε_{475}=2.14×10^4 M^{-1}cm^{-1}, and ε_{490}=2.08×10^4 M^{-1}cm^{-1}) determined from the intercept. These results suggest that the sixteen sites are spectrophotometrically equivalent with each other.

Temperature-Jump Relaxations. The temperature-jump measurements revealed that the interaction between Orange I and BSA was characterized by five relaxation processes. Some typical relaxation curves

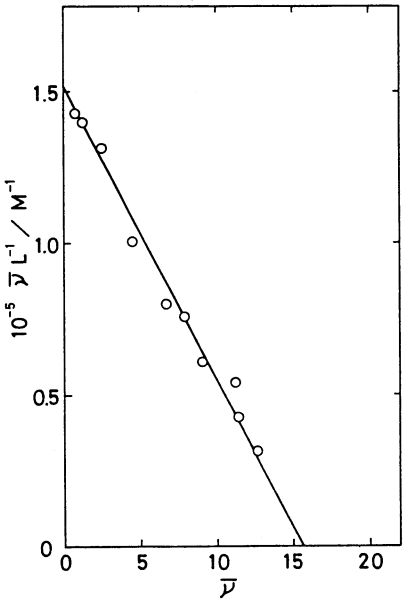

Fig. 1. Scatchard plot of the interaction of Orange I with BSA at 25°C and pH=7.0. The solid line represents the least-square fit to the data.

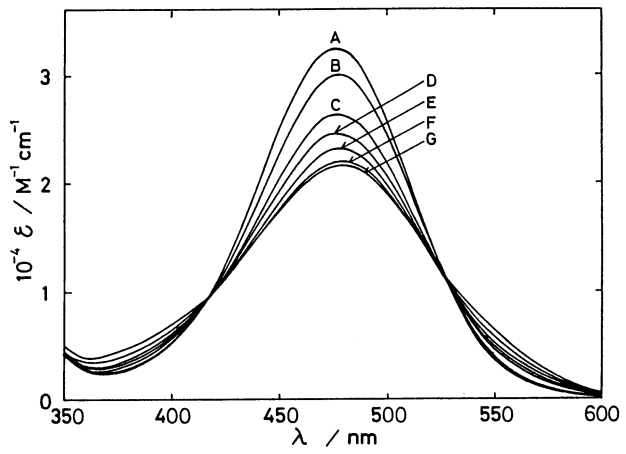

Fig. 2. Absorption spectra of Orange I in the presence of BSA at several concentrations. The data were obtained at 25°C, pH=7.0 and L_0=1.00×10^{-5}M. A: dye only, B: P_0=1.82×10^{-6}M, C: P_0=9.10×10^{-6}M, D: P_0=1.82×10^{-5} M, E: P_0=3.64×10^{-5}M, F: P_0=9.10×10^{-5}M, G: P_0=1.82×10^{-4}M.

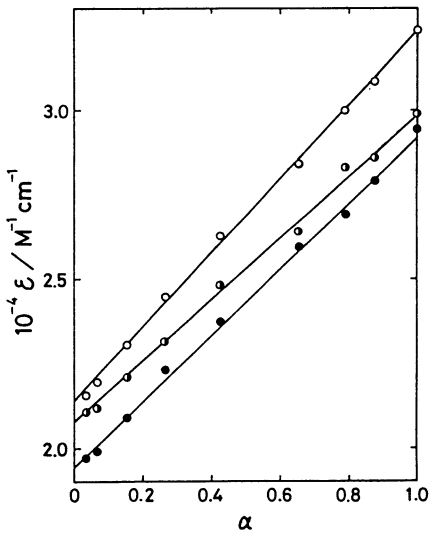

Fig. 3. Plots of ε vs. α at 460 nm (●), 475 nm (○), and 490 nm (◑). The solid lines represent least-square fits to the data.

observed at L_0/P_0 (ligand to protein ratio)=2 are shown in Fig. 4. The data were obtained at either 475 nm or 555 nm so as to give a good signal-to-noise ratio. The fastest relaxation (Fig.4(A)) was characterized by a single relaxation time (τ_1), while the second (Fig. 4(B): τ_2 and τ_3) and the third (Fig. 4(C): τ_4 and τ_5) were

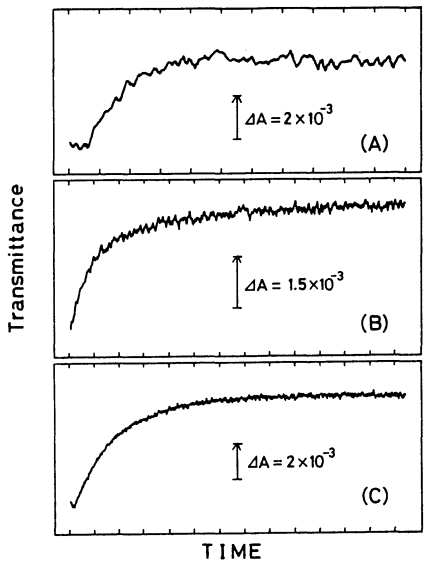

Fig. 4. Typical relaxation curves observed for the Orange I-BSA system at 25°C , pH=7.0, P_0= 5×10^{-5} M, and L_0/P_0=2. (A) λ=555 nm, 5 μs per division, (B) λ=555 nm, 1 ms per division, (C) λ=475 nm, 20 ms per division. The arrow designated for each curve shows the magnitude and the direction of the positive absorbance change.

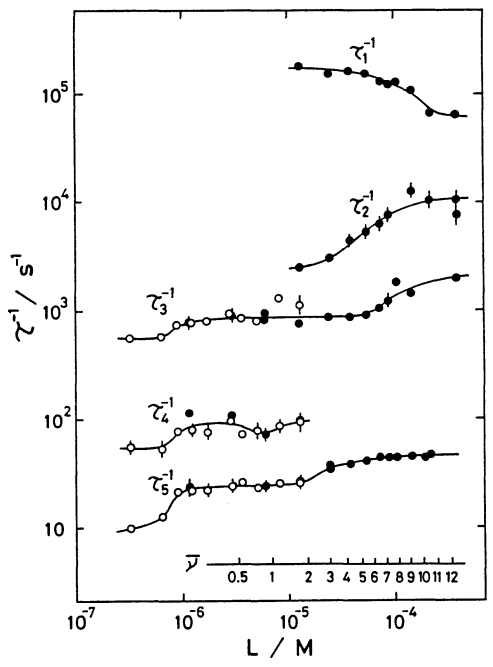

Fig. 5. Plots of τ^{-1} vs. L. The data were collected for two kinds of concentration dependence: (○) P_0/L_0 dependence (from 0.2 to 20) at $L_0=2\times10^{-5}$ M, (●) L_0/P_0 dependence (from 0.2 to 20) at $P_0=5\times10^{-5}$ M. The scale of $\bar{\nu}$ is also designated at the bottom of the figure.

double relaxations. To cover a wide range of reactant concentrations, the relaxation time of each process was determined for two kinds of concentration dependence: (1) P_0/L_0 dependence at $L_0=2\times10^{-5}$ M and (2) L_0/P_0 dependence at $P_0=5\times10^{-5}$ M. Figure 5 shows a plot of the reciprocal relaxation times versus the free-ligand concentration (L) as well as versus the $\bar{\nu}$ values, which were calculated using the values of n and K determined from the equilibrium dialysis measurement. It can be seen from this figure that the reciprocal relaxation times are increasing functions of L, except in the case of τ_1^{-1}. Furthermore, it can be seen that τ_4^{-1} disappears above $\bar{\nu}$=2 and that, in the same region, τ_2^{-1} becomes observable.

Reaction Scheme. Although the scheme of Eq. 2 is consistent with the equilibrium dialysis and the spectrophotometric data, it is obvious that this scheme is too simple to interpret the observed multiple relaxation and that it is not applicable to the present kinetic data.

Almost all the kinetic studies of albumin-ligand interaction have been concerned with specific ligands, such as bilirubin,[3,4] hemin,[7] fatty acids,[5] warfarin,[6] and Bromphenol Blue,[8] which have one strong or extremely strong primary binding site on the albumin molecule. Moreover, the data were collected over the reactant concentration range where only the primary binding occurs. A common feature of the schemes established by these studies is that a rapid bimolecular binding is followed by subsequent unimolecular stabilizations of the complex. That is,

$$\mathrm{L+S} \rightleftarrows \mathrm{C_1} \rightleftarrows \mathrm{C_2} \rightleftarrows \cdots \rightleftarrows \mathrm{C_m} \qquad (5)$$

This type of scheme predicts the reciprocal relaxation time for the i th isomerization as:[13]

$$\tau_i^{-1} = k_i + k_{-i} \qquad (6)$$

in the case of a rapid isomerization between slow ones or:

$$\tau_i^{-1} = k_i \frac{E\,(L+S)}{1+F\,(L+S)} + k_{-i} \qquad (7)$$

in the case of an isomerization slower than the preceding steps. In these equations, k_i and k_{-i} are the forward and backward rate constants of the ith step respectively, while E and F are functions of the equilibrium constants of the preceding steps. According to these equations, the reciprocal relaxation time for any of the isomerization steps must be concentration-independent or an increasing function of $L+S$. Based on a calculation using the binding parameters determined from the dialysis measurements, it can be seen that $L+S$ decreases with the increase in L at $L<7\times10^{-4}$ M, the area where almost all the relaxations were measured. Therefore, Fig. 5 shows that the reciprocal relaxation times of the four slower processes are decreasing functions of $L+S$. That is, Eq. 5 also is not applicable to the present system.

To obtain an insight into the binding scheme, we must take notice of the fact that the reciprocal relaxation times (τ_3^{-1}, τ_4^{-1}, τ_5^{-1}) are functions of only L. This fact suggests the following basic scheme for one of the relaxation times:[14]

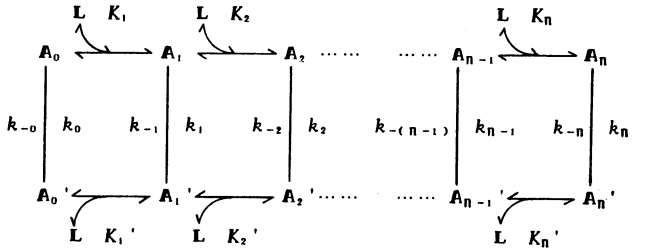

(8)

where $\mathbf{A}_i$ and $\mathbf{A}_i'$ are two isomeric forms of BSA which bind i ligands and where K_i and K_i' are association constants to form two ith complexes, $\mathbf{A}_i$ and $\mathbf{A}_{i-1}$, from $\mathbf{A}_{i-1}$ and $\mathbf{A}_{i-1}$ respectively, and where n is the maximum number of bound ligands. The equilibrium between $\mathbf{A}_0$ and $\mathbf{A}_0'$ ($\mathbf{A}_0 \rightleftharpoons \mathbf{A}_0'$) represents a mode of isomerization in the absence of a ligand, which shifts to $\mathbf{A}_1 \rightleftharpoons \mathbf{A}_1'$, $\mathbf{A}_2 \rightleftharpoons \mathbf{A}_2'$, ·····, and finally to $\mathbf{A}_n \rightleftharpoons \mathbf{A}_n'$ with the increase in the number of bound ligands. k_i and k_{-i} are the forward and backward rate constants of the ith isomerization. Assuming that bimolecular bindings are rapid compared with the isomerizations and that the concentration changes of L are negligible during the slow isomerizations, the reciprocal relaxation time for the slow steps becomes:[14]

$$\tau^{-1} = \frac{k_0 + k_1K_1L + k_2K_1K_2L^2 + \cdots\cdots + k_nK_1K_2\cdots K_nL^n}{1 + K_1L + K_1K_2L^2 + \cdots\cdots + K_1K_2\cdots K_nL^n} + \frac{k_{-0} + k_{-1}K_1'L + k_{-2}K_1'K_2'L^2 + \cdots + k_{-n}K_1'K_2'\cdots K_n'L^n}{1 + K_1'L + K_1'K_2'L^2 + \cdots\cdots + K_1'K_2'\cdots K_n'L^n} \quad (9a)$$

$$= \frac{k_0A_0 + k_1A_1 + k_2A_2 + \cdots\cdots + k_nA_n}{A_0 + A_1 + A_2 + \cdots\cdots + A_n} + \frac{k_{-0}A_0' + k_{-1}A_1' + k_{-2}A_2' + \cdots\cdots + k_{-n}A_n'}{A_0' + A_1' + A_2' + \cdots\cdots + A_n'} \quad (9b)$$

As can be seen in Eq. 9a, τ^{-1} is expressed as a function of L alone, in agreement with the present data (Fig. 5). On the other hand, Eq. 9b shows that τ^{-1} is the apparent rate constant of the isomerization , averaged over the existing complex species. At the limit of dilution, Eq. 9a can be approximated by k_0+k_{-0}. With an incease in L, the terms of the higher powers of L in both the numerator and the denominator in Eq. 9a become significant. If the terms of the ith power of L are predominant, Eq. 9a can be approximated as $\tau^{-1}=k_i+k_{-i}$ (apparent rate constant of the isomerization of the ith complex). That is, the τ^{-1} of Eq. 9 follows the rate of the isomerization of predominantly existing complexes at a given ligand concentration.

On the basis of these considerations, we may construct a scheme applicable to the present kinetic data:

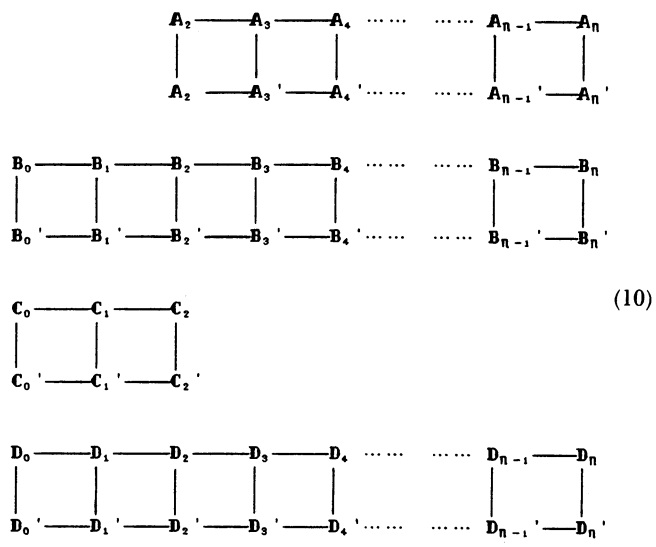

(10)

where $\mathbf{A}_i \rightleftharpoons \mathbf{A}_i'$, $\mathbf{B}_i \rightleftharpoons \mathbf{B}_i$, $\mathbf{C}_i \rightleftharpoons \mathbf{C}_i'$, and $\mathbf{D}_i \rightleftharpoons \mathbf{D}_i'$ represent the four modes of isomerization which are characterized by the relaxation times of τ_2, τ_3, τ_4, and τ_5 respectively. The horizontal lines are steps of the ligand binding, where the symbols associated with the ligand (see Eq. 8) are dispensed with. According to this scheme, the observed data may be interpreted as follows.

In the absence of a ligand, there are three intrinsic modes of isomerization, designated by $\mathbf{B}_0 \rightleftharpoons \mathbf{B}_0'$, $\mathbf{C}_0 \rightleftharpoons \mathbf{C}_0'$, and $\mathbf{D}_0 \rightleftharpoons \mathbf{D}_0'$. The apparent rate constants of these modes can be evaluated from the asymptotic values of τ_3^{-1}, τ_4^{-1}, and τ_5^{-1} within the limits of the diluted ligand concentrations (Fig. 5) as 570, 55, and 7—8 s^{-1} respectively. With an increase in the concentration of free ligands, these modes shift toward those of the complex species, accompanying the increase in the apparent rate constants. At the ligand concentration where $\bar{\nu}>2$, Mode C ceases to be observable; instead, Mode A appears at a very rapid rate. This implies that the binding of two ligands freezes Mode C by displacing the equilibrium almost completely to either of the isomers or, by inducing some kind of conformational change in the complex, alternatively causes another fast mode (Mode A). With a further increase in L, the apparent rate constants increase further and reach plateau values. It may be worth noting that the relaxation amplitude of each mode has a maximum at a $\bar{\nu}$ value between 4 and 6.5 and that this relaxation amplitude decreases (Modes B and D) or increases (Mode A) with a further increase in L, suggesting that Mode A is the most predominant mode at high $\bar{\nu}$ values.

Contrary to the case of the slower relaxations, τ_1^{-1} decreases with the increase in L (Fig. 5); that is, it increases with $L+S$. Considering the very rapid rate as well, this behavior may be interpreted by attributing the relaxation to the bimolecular binding step between the free ligand and the free binding site, such as in Eq. 2. The reciprocal relaxation time for the binding step

becomes:

$$\tau_1^{-1} = k_a(L+S) + k_d \quad (11)$$

where k_a and k_d are the rate constants of association and dissociation respectively. Figure 6 shows the plot of τ_1^{-1} vs. $L+S$, which was calculated using these binding parameters: $n=16$ and $K=9.7\times10^3$ M^{-1}. In agreement with Eq. 11, the plot shows a linear dependency in the region where τ_1^{-1} is larger than 1.2×10^5 s^{-1} and where $\bar{\nu}$ is smaller than 8. The deviation from the linearity at $\bar{\nu}>8$ may arise from interactions between sites attributable to some kind of conformational change in the complex. The slope and the intercept of the plot yield $k_a=2.4(\pm0.5)\times10^8$ $M^{-1}s^{-1}$ and $k_d=1.0(\pm2.9)\times10^4$ s^{-1} respectively. From these values, the binding constant can be calculated as $K=k_a/k_d=2.4\times10^4$ M^{-1}. Considering the estimated errors, this value may be regarded as consistent with the binding constant used for this analysis. This self-consistency confirms the present assignment for τ_1.

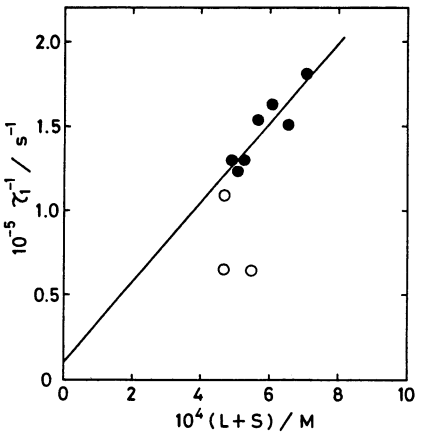

Fig. 6. Plot of τ_1^{-1} vs. $L+S$. The solid line represents the least-square fit to the data (filled circles) in the region where $\bar{\nu}<8$. Open circles show the data observed at $\bar{\nu}>8$.

Role of Isomerization Modes in Ligand-Binding Mechanism. Karush,[1] in 1950, proposed a concept of the "configurational adaptability" of albumin molecules in order to interpret their unique capability in the binding of diverse kinds of ligands. By this term, he meant that an albumin molecule in an aqueous solution is not a single form but an ensemble of many structural species in equilibrium with each other and of approximately equal energies. In the presence of a ligand, the isomeric form is stabilized by preferential interaction with the ligand, resulting in a stable complex. On the other hand, Kragh-Hansen, in his review[2] of ligand binding to serum albumin, pointed out another possibility for the binding mechanism. Many previous kinetic studies have revealed this general binding scheme (Eq. 5): a very rapid bimolecular binding, followed by sequential stabilization processes. This scheme has led him to propose a "pronounced flexibility" mechanism: a ligand molecule is, during the binding process, able to modify the configuration of a binding region so as to produce a greater congruence between the ligand molecule and parts of the region. The present scheme (Eq. 10), however, shows that BSA has, in the absence of a ligand, three modes of conformational change between isomeric forms in equilibrium. The addition of a ligand shifts the set of modes toward that of the complex species accompanying rate change, mode freezing, and the production of another mode. This behavior may be interpreted as the response of the system aimed at acquiring the most stable state as the pressure of the

Table 1. Rates of Isomerization Steps Observed for Albumin-Ligand Systems

System[a]	Rate/s^{-1}				Condition		Ref.
	(Mode A)	(Mode B)	(Mode C)	(Mode D)	T/°C	pH	
BPB-BSA		400—600	40	1—3	25	7.0	8
BCP-BSA		100—600			25	5.3—6.8	15
PR-BSA	5×10^3			3	30	7.35	16
			10—50	4—6		7.0	16
HABA-BSA		200			25	7.0	17
Long-chain fatty acid-HSA				3			5
ANS-BSA		125			25	7.0	18
Warfarin-HSA			60		25	8.7	19
			55	2.5—5	25	6.0	20
			74			9.0	20
			10—60		25	6—9	21
Bilirubin-BSA				8.5	23	7.4	22
Hemin-HSA				6.3	24	7.0	7
BPA E,F→N			50	4	25		23
BSA CD change				4—10	22	7.5—9	24
Orange I-BSA	2.5×10^3—10^4	570	55	7—8	25	7.0	This work

a) Abbreviations: BPB=Bromphenol Blue, BCP=Bromcresol Purple, PR=Phenol Red, HABA=2-(4-hydroxyphenylazo)benzoic acid, HSA=human serum albumin, ANS=8-anilino-1-naphthalenesulfonic acid, BPA=bovine plasma albumin, E,F→N=pH-jump from E and F states to the N state of albumin.

ligand concentration increases. This seems to be just the case with the configurational adaptability in the sense of Karush.

Table 1 lists the rates of the isomerization steps of complex formation reported for albumin-ligand systems at around 25 °C and in the neutral-pH region, as well as those of conformational transitions observed under similar conditions. It can be seen from this table that (1) there are four modes of isomerization, which may be classified according to the rate as: A (10^3—10^4 s^{-1}), B (10^2—10^3 s^{-1}), C (10—10^2 s^{-1}), and D (1—10 s^{-1}); (2) the number of observable modes depends on the ligand species, and finally (3) the rates, i.e., the activation free energies, which belong to a mode for different ligands are all similar to each other, regardless of the structure of the ligand. Kuwajima et al.,[23] by studying the pH-jump from the E and F states to the N state[25] of albumin molecules, observed time-dependent absorbance changes at 296 nm which are characteristic of the ionization states of tyrosyl residues. The rates of these changes (50, 4 s^{-1}), listed in Table 1, agree well with those classified in Mode C and Mode D for albumin-ligand systems. Using a pressure-jump technique with circular dichroism (CD) detection, Gruenewald and Knoche[24] observed a CD change at 222 nm. Its rate (4—10 s^{-1}) is classifiable in Mode D (Table 1). This fact suggests that Mode D is an isomerization which accompanies a change in the helix content of albumin molecules. From the pH-dependence of the rates of Mode D in the Phenol Red-BSA system,[16] Mode C in the warfarin-HSA system,[21] and the Mode D observed by the pressure-jump CD measurement,[24] it can be seen that these modes are closely related to the N⇄B transition[25] of albumin molecules. Mode A and Mode B have not been well characterized from the point of view of the conformational state of the protein. Because Mode A was observed only at high L_0/P_0 values, it is not necessarily attributable to an isomerization of native albumin, but seems to arise from the albumin-ligand complex. There may also be another slow mode of isomerization ($\tau^{-1}<1$ s^{-1}),[23,26] but it is not discussed in the present paper.

These observations suggest that the modes of isomerization of pure albumin molecules are closely related to the ligand-binding mechanism. In the absence of a ligand, albumin molecules are distributed among many structural species, each of which is characterized by a set of isomers of those modes, and the structures of the albumin molecules fluctuate between those species on several time scales and to several spatial extents. Immediately after the addition of a ligand, and before the fastest mode of isomerization takes place, the ligand molecules will at first come into a rapid binding equilibrium with the instantaneous structural species. In this stage, extremely fast (faster than, or comparable to, the relaxation time of the diffusion-controlled bimolecular binding process) rearrangements of the side chains and mobile segments in the vicinity of the binding site slightly stabilize each of the isomeric forms and also slightly alter the free-energy profile of each mode. Because of the time limitation, possible structural changes must be restricted to a very local region of the protein molecule. The alteration is, therefore, probably so small that the free-energy profile and the distribution of albumin molecules among the structural species are essentially the same as those in the pure albumin solution. In the second stage, the ligand molecules will come into an equilibrium with the fastest mode of isomerization. At this stage, albumin molecules are able to use slower and larger structural changes than those in the previous step to establish a preferable interaction with ligand molecules. Each of the isomers of the fastest mode may be stabilized by the structural changes, but they may be destabilized if such a preferable interaction can not be attained because of structural restrictions, resulting in an alteration of the free-energy profile along the reaction coordinate of the fastest mode. If the activation free energy is lowered, the rate of the isomerization becomes fast and the redistribution of the complex species among the isomers is achieved through the altered mode. On the other hand, if the activation free energy becomes large, the rate becomes slow and the redistribution will be achieved mainly through the mode of pure albumin. Within the limits of a large activation free energy, however, this mode is practically prohibited. Furthermore, it may also be possible that a strong interaction between ligand and binding site causes some kinds of conformational transitions of albumin molecules and extinguishes the mode of isomerization, alternatively causing another, new isomerization mode. In each subsequent equilibration step, similar changes will occur along another reaction coordinate in still larger spatial and slower time scales, keeping the equilibrium in the faster modes. When all the modes come into an equilibrium with the ligand molecules, a stable distribution of the complexes is established. In the case of the present system, it is likely that the activation free energy of each mode is progressively lowered with the increase in the number of bound ligands and that some kinds of conformational change take place when two ligand molecules are bound. Some kinds of ligand molecules may interact selectively with either of the isomers. Even in such a case, though, it is also possible that the stabilization of the complex takes place through the reaction coordinates of the isomerization modes; that is, a bimolecular binding step is followed by subsequent unimolecular isomerizations (Eq. 5). This may correspond to the case of the interaction between albumin and such specific ligands as bilirubin.[3,4] In this way, the existence of the isomerization modes of albumin molecules may be closely connected with the formation of stable albumin-ligand complexes.

References

1) F. Karush, *J. Am. Chem. Soc.*, **72**, 2705 (1950).
2) U. Kragh-Hansen, *Pharmacol. Rev.*, **33**, 17 (1981).
3) T. Faerch and J. Jacobsen, *Arch. Biochem. Biophys.*, **184**, 282 (1977).
4) R. D. Gray and S. D. Stroupe, *J. Biol. Chem.*, **253**, 4370 (1978).
5) W. Scheider, *Proc. Natl. Acad. Sci. U.S.A.*, **76**, 2283 (1979).
6) N. Rietbrock and A. Laβmann, *Naunyn-Schmiedeberg's Arch. Pharmacol.*, **313**, 269 (1980).
7) P. A. Adams and M. C. Berman, *Biochem. J.*, **191**, 95 (1980).
8) K. Murakami, T. Sano, and T. Yasunaga, *Bull. Chem. Soc. Jpn.*, **54**, 862 (1981).
9) R. F. Chen, *J. Biol. Chem.*, **242**, 173 (1967).
10) E. J. Cohn, W. L. Huges, Jr., and J. H. Weare, *J. Am. Chem. Soc.*, **69**, 1753 (1947).
11) K. Murakami, K. Mizuguchi, Y. Kubota, and Y. Fujisaki, *Bull. Chem. Soc. Jpn.*, **59**, 3393 (1986).
12) G. Scatchard, *Ann. N. Y. Acad. Sci.*, **51**, 660 (1949).
13) C. F. Bernasconi, "Relaxation Kinetics," Academic Press, New York (1976), p. 40.
14) H. Strehlow and W. Knoche, "Fundamentals of Chemical Relaxation," in "Monographs in Modern Chemistry," ed by H. F. Ebel, Verlag Chemie, New York(1977), Vol. 10, pp. 85—90.
15) Z. Horiuchi, M. Nakao, S. Abe, K. Takahashi, and T. Yasunaga, *J. Sci. Hiroshima Univ., Ser. A*, **39**, 37 (1975).
16) D. E. Goldsack and P. M. Waern, *Can. J. Biochem.*, **49**, 1267 (1971).
17) K. Murakami, T. Sano, T. Tsuchie, and T. Yasunaga, *Biophys. Chem.*, **21**, 127 (1985).
18) H. Nakatani, M. Haga, and K. Hiromi, *FEBS Lett.*, **43**, 293 (1974).
19) J. Wilting, J. M. H. Kremer, A. P. Ijzerman, and S. G. Schulman, *Biochim. Biophys. Acta*, **706**, 96 (1982).
20) A. Laßmann and N. Rietbrock, *Naunyn-Schmiedeberg's Arch. Pharmacol.*, **320**, 189 (1982).
21) J. M. H. Kremer, G. Bakker, and J. Wilting, *Biochim. Biophys. Acta*, **708**, 239 (1982).
22) R. F. Chen, *Arch. Biochem. Biophys.*, **160**, 106 (1974).
23) K. Kuwajima, T. Matsushima, K. Nitta, and S. Sugai, *Biopolymers*, **23**, 1347 (1984).
24) B. Gruenewald and W. Knoche, *Rev. Sci. Instrum.*, **49**, 797 (1978).
25) J. F. Foster, "Albumin Structure, Function and Uses," ed by V. M. Rosenoer, M. Oratz, and M. A. Rothschild, Pergamon Press, New York (1977), pp. 53—84.
26) E. S. Benson, B. E. Hallaway, and R. W. Lumry, *J. Biol. Chem.*, **239**, 122 (1964).